Multicrystalline silicon thin film solar cells based on vanadium oxide heterojunction and laser doped contacts

Isidro Martín[*1], Gema López[1], Jonathan Plentz[2], Chen Jin[1], Pablo Ortega[1], Cristóbal Voz[1], Joaquim Puigdollers[1], Annett Gawlik[2], Guobin Jia[2], Gudrun Andrä[2]*

[1] Departament d'Enginyeria Electrònica, Universitat Politècnica de Catalunya, Jordi Girona 1-3, Barcelona 08034, Spain

[2] Leibniz Institute of Photonic Technology (IPHT), Albert-Einstein-Str. 9, 07745 Jena, Germany

Keywords: LPC silicon, IBC solar cell, laser doping, selective contacts.

Abstract

Liquid phase crystallized (LPC) silicon thin films on glass substrates are a feasible alternative to conventional crystalline silicon (c-Si) wafers for solar cells. Due to substrate limitation, a low temperature technology is needed for solar cell fabrication. While silicon heterojunction is typically used, in this work the combination of vanadium oxide/c-Si heterojunction as emitter and base contacts defined by IR laser processing of phosphorus-doped amorphous silicon carbide stacks is explored. LPC solar cells are fabricated using such technologies in order to identify their issues and advantages with a promising performance of an active-area efficiency of 5.6%. Apart from the absence of light trapping techniques, the relatively low efficiency obtained is attributed to a low lifetime in the LPC silicon bulk. These poor material properties imply a short diffusion length that makes that only photogenerated carriers in the emitter regions could be collected. Consequently, future devices should show narrower base contact regions, suggesting a shorter-wavelength laser, combined with longer LPC substrate lifetimes.

1. Introduction

Crystalline silicon (c-Si) photovoltaic technology is always pursuing to be more efficient and environmental compatible with the final objective to be an attractive in front of conventional energy sources. As an alternative to wafer-based c-Si photovoltaic devices, liquid-phase crystallized (LPC) thin film silicon on glass technology has been proposed in a laboratory scale. In this technology, amorphous silicon is deposited on glass and subsequently recrystallized by a line focused laser beam [1-3] or an electron beam.[4-5] The resulting multi-crystalline thin film silicon is ready for the definition of emitter and base contacts in an interdigitated back-contacted (IBC) structure at the rear surface using a low temperature approach. Up to now, the most efficient devices fabricated on LPC substrates use silicon heterojunction technology,[6-7] together with bifacial concepts.[8]

Recently, heterojunction between c-Si and transition metal oxides have been proposed to be an alternative to the well-known amorphous/crystalline silicon heterojunction approach.[9-10] This new technology avoids the usage of toxic and/or flammable dopant gas precursors with comparatively lower temperature processing. In particular, excellent results have been reported for IBC c-Si solar cells fabricated using vanadium oxide (VO_x) as hole transport layer while the n-type base contacts are defined by laser processing of phosphorus doped amorphous silicon carbide stacks.[11] In this work, we explore the viability of this technology when it is applied to LPC substrates with the objective of identifying the main advantages and issues of the structure.

2. Experimental

LPC substrates were fabricated using 3.3 mm thick Borofloat 33 (Schott) glasses. An 80 nm silicon nitride (SiN_x) layer is deposited on glass as barrier layer followed by electron

beam evaporation of phosphorus doped silicon (6.8 μm). Next, this material is recrystallized by scanning it with a continuous wave diode laser[12] at 808 nm resulting in an n-type multicrystalline silicon with donor density of $1.5 \cdot 10^{17}$ cm^{-3}. Based on these substrates, we fabricate the solar cells following the fabrication process shown in **figure 1,(a)**. After an RCA cleaning, a 50 nm aluminium oxide (Al_2O_3) film is deposited by Atomic Layer Deposition on the rear surface to passivate it.[13-14] This film is then covered with 45 nm of stoichiometric silicon carbide (SiC) deposited by PECVD in order to protect it from the subsequent chemical etchants and cleaning steps.[15] This dielectric stack (Al_2O_3/SiC) is patterned by photolithography to open stripe-like regions where the phosphorus doped amorphous silicon carbide (SiC_x(n)) stack was deposited. This stack provides surface passivation and the dopant source for the laser doping process that creates the base contacts.[16] Next, rear surface is again patterned and cleaned to prepare it for the deposition of the emitter. In this case, we thermally evaporated vanadium oxide (VO_x) and contact it by indium tin oxide (ITO) following the technology developed in ref. [10]. Once the emitter layers were removed from the base contact regions, we laser processed them creating point-like contacts of about 60 μm of diameter separated with a distance of 200 μm using a Nd:YAG laser source at 1064 nm with 1.1 mW and 6 pulses per spot.[16] Finally, we evaporated by electron beam a contact consisting of 40 nm of titanium and 1 μm of aluminum and we define separated fingers by photolithography. It should be mentioned that the metallization of the emitter region is different from the one reported in ref. [11]. In that work, a two-level metallization with Ni/Al on the VO_x and only Al on the base contacts was used. Despite the good results, that structure is very challenging from the point of view of fabrication process. For the sake of simplicity, we followed the simpler approach described above with Ti/Al for both contacts following the results reported in ref. [16-

17]. The final device has a total area of 16.8 mm^2 (4.2x4 mm^2) with emitter width of 1000 μm and distance between base fingers or pitch of 1400 μm. Consequently, the active area is 12 mm^2. A picture of the fingers in the final device together with a sketch of its cross-section can be seen in **figure 1 (b)**.

3. Results

As a first characterization, we measure the dark current density (J) vs. voltage (V) curve shown in **figure 2**. As it can be seen, the curve shows a rectifying factor of more than 5 orders of magnitude indicating that an energy barrier is created at the VO_x/c-Si interface. In that curve, two exponential trends can be seen. In order to characterize it, we calculate the local ideality factor (n_{loc}) as:

$$n_{loc} = \frac{q}{k_B T} \cdot \frac{1}{\delta \ln J / \delta V} \quad (1)$$

Results shown in the inset of figure 2 indicate n_{loc} values in the range of 2.5-3 which are much higher than the 1.2 value reported in ref. [11] with a similar structure on FZ c-Si wafers. Given the difference in substrate quality between both devices and the low carrier lifetimes measured at LPC substrates,[18] we suggest that the main recombination is located at material bulk with a strong dependence of the bulk lifetime on carrier injection that could be behind the high measured ideality factors.

In **Table I,** the photovoltaic parameters of the solar cell measured under 1 sun-illumination with AM1.5g are shown. The open-circuit voltage (V_{oc}) value is strongly dependent on material quality and previous works based on similar Si thin films than the ones used hereby demonstrated implied open-circuit voltage in the range of 550 mV.[18] Consequently, we think that this value is limited by absorber quality and it is not inherent to the solar cell structure.

Regarding fill factor (*FF*), suns- V_{oc} measurements were carried out in order to calculate the pseudo-fill factor (*pFF*). These measurements are not impacted by ohmic losses and *pFF* is considered as the *FF* limited by the ideality of the current mechanism behind the junction. For our sample, assuming a unique exponential trend with ideality factor equal to 1, the maximum reachable *FF* value, also known as ideal Fill Factor (FF_0) , is 81.7 %. The measured *pFF* value is 66.4 % which is much lower than the calculated FF_0 indicating that the current mechanism has an ideality factor much higher than 1. This result agrees with the values of n_{loc} deduced from the dark J-V curve (see figure 2). On the other hand, the *pFF*-*FF* difference allows us to calculate the series resistance (R_s) at the maximum power point following the expression:[19]

$$R_s = \left(1 - \frac{FF}{pFF}\right)\frac{V_{oc}}{J_{sc}} \tag{2}$$

The resulting R_s value is in the range of 10.3 Ω·cm^2. Through Quokka 2 simulations,[20] for the case of ideal contacts we obtain a series resistance lower than 1 Ω·cm^2 in a solar cell that reproduces the geometrical structure of our rear contacts. Then, the contact geometry used in the solar cell is not responsible for the high series resistance. However, the impact of the laser processing on such thin c-Si substrates is not accurately characterized. The IR wavelength used implies a high thermal load to the thin film silicon that must be dissipated by a much lower quantity of material than the one found for the usual thick wafer substrates. This could lead to distortions in dopant redistribution and/or in surface passivation at the laser spot surroundings. Then, further research is needed to accurately quantify the effect on ohmic losses due to the local laser doped contacts onto these particular thin film devices in order to clarify the origin of the high R_s measured value.

Finally, the obtained short-circuit current density (J_{sc}) values are lower than expected and they are the main reason limiting solar cell efficiency. As it can be seen in Table I, a J_{sc} of 13.62 mA/cm^2 is measured for flat surfaces and adding a texturized PDMS foil on top of the glass in order to improve optical properties[21] J_{sc} increases to 14.40 mA/cm^2. As a result, a maximum efficiency of 4.0 % is measured. In order to clarify the origin of such low J_{sc} values, Laser Beam Induced Current (LBIC) measurements were carried out using a laser at λ= 544 nm with a scan resolution of 50×50 μm^2. The External Quantum Efficiency (EQE) mapping is shown in **figure 3** where we can see that only the emitter regions are contributing to carrier collection. Consequently, taking into account this effect J_{sc} can be calculated using the active area instead of aperture area which results in 19.07 mA/cm^2 without PDMS foils and 20.16 mA/cm^2 with it. These values agree with previous thin film solar cells fabricated by our research group [22-23] and lead to an active-area efficiency of 5.6 %. It must be mentioned that these values are reached without texturing silicon surface to enhance the light trapping introducing remarkable optical losses at longer wavelengths.[3]

The LBIC results can be explained through the minority carrier diffusion length. This parameter determines the mean path that minority carriers (holes) can travel before recombining. The expected carrier diffusion length in the silicon thin film absorbers is in the range of several 10 μm which is long enough to collect minority carriers in the thin (below 10 μm) absorbers when they are photogenerated over the emitter regions. [24-25] On the contrary, photogenerated carriers out of these regions are further away from the collector contact recombining in the material bulk and, thus, base contact regions are not active for carrier collection. Moreover, the lateral transport of minority carriers is jeopardized by the high density of grain and twin boundaries observed.[3]

Once we have identified the main issues in carrier collection, we can get a deeper insight by analysing EQE measurements. These measurements were carried out with a light spot of 2.8×2.8 mm^2 covering both emitter and base contact regions. Then, knowing that base contact regions are not contributing into the carrier collection, we can assign the EQE data only to the emitter regions and apply their area fraction into the experimental data leading to the EQE of the emitter regions. Taking into account only emitter regions allows us to model carrier collection by PC-1D defining a very thin emitter at the rear surface of a piece of c-Si with the corresponding absorber thickness (6.8 μm). Refractive index and thickness of the front layers are also included in the simulations. With this structure, the only three free parameters are the front surface recombination velocity (S_{front}), the bulk lifetime (τ_B) and the rear internal reflectance (R_{rear}). **Figure 4** shows EQE experimental data and their fitting by PC-1D simulations. Regarding rear internal reflectance, it impacts EQE on the soft decay beyond λ= 600 nm and an accurate fitting is obtained for R_{rear}= 65 %, as shown in figure 4. For shorter wavelengths, good fitting of the experimental curve is obtained with S_{front}< 1000 cm/s and τ_B= 0.08-0.1 μs. This bulk lifetime value agrees well with previous works on similar substrates.[24,25] Moreover, using this range for τ_B and a hole diffusion constant of 7.34 cm^2/s, we calculate a diffusion length range of 7.66-8.56 μm. This range agrees well with the discussion above being longer than the substrate thickness and too short to collect carriers out of the emitter contact regions. The EQE curve also shows the influence of the missing light trapping, which is mandatory for thin film silicon solar cells, but not included in this first approach solar cell with VO_x hetero-emitter and laser doped base contacts.

4. Discussion

After the device characterization explained above, we can conclude that heterojunction emitters based on transition metal-oxides, like VO_x, are viable for LPC silicon thin film leading to lower temperature and more environmentally friendly devices. However, the main limitation of the fabricated structure is related to the relatively wide dimensions of the base contacts defined by laser doping and its comparison to the diffusion lengths expected in these thin film materials. There are two main strategies to solve this problem. On the one hand, the width of the base contact regions could be reduced to be shorter than the diffusion length. For laser doping contacts, it means that laser spot on c-Si should shrink which probably implies a change of the laser source to shorter wavelengths, as the one reported in ref. [26] where laser spots have a diameter of ~30 μm using a UV laser. Additionally, this UV laser source could lead to shallower effects onto thin mc-Si substrates that could help in keeping good material and surface properties at the laser spot surroundings. On the other hand, material quality could be improved by optimizing the laser recrystallization process together with the barrier layer. This layer plays a key role in substrate performance by different mechanisms: it must work as a barrier for impurity diffusion from the glass during laser recrystallization; it must prevent dewetting during the liquid silicon melting process and, consequently, it has a significant impact on solidification and crystallization process, i.e. crystal quality. Finally, it must also passivate the front surface in the final device. From the point of view of carrier collection, the requirement is to have diffusion lengths longer than half of the distance between emitter regions. If this condition was fulfilled, photogenerated carriers out of the emitter regions could be collected. Lifetime values in the range of a few microseconds are reported in the literature[6-7] leading to diffusion lengths of ~50 μm. Consequently, a combination of

both strategies could be a feasible solution to fully exploit the potential of laser doped contacts on LPC thin films. Additionally, the insertion of a suitable light trapping for the reported concept would also increase the efficiency.[24]

5. Conclusions

In this work, we report on solar cell results on LPC thin film silicon with emitters based on VO_x/c-Si heterojunctions and laser-doped base contacts as a proof-of-concept device. Best solar cell results are V_{oc}= 558 mV, J_{sc}= 14.40 mA/cm^2 and FF= 49.6 % leading to an efficiency of 4.0 %. The low FF could be attributed to a non-ideal current mechanism together with high ohmic losses probably related to the laser processed contacts. On the other hand, low J_{sc} is explained by the fact that no light trapping is introduced in the planar thin films and only photogenerated carriers on the emitter regions are collected, as demonstrated by LBIC measurement. Considering only that active area is collecting carriers, a more representative value of cell performance is the active-area efficiency which results in 5.6 %. A short diffusion length is deduced from the EQE measurement which explains the loss of photogenerated carriers out of the emitter regions. After analysing these results, a combination of smaller laser spots with better material properties and additional light trapping techniques could be a feasible strategy to fully exploit the potential of the solar cell concept proposed hereby.

Acknowledgements

This work was funded by MINECO from Spanish government under projects TEC2017-82305-R and ENE2017-87671-C3-2-R. The authors acknowledge the financial support by Thüringer Aufbaubank (TAB) for the project "Bi-PV" (FKZ: 2015 FGR 0078) and the European Social Fund (ESF) for co-funding this project, and resource from the MSC-Action “cSiOnGlass” under contract number GA 657115 by the European

Commission has been used. The authors thank Dr. Michael Vetter (formerly at Leibniz Institute of Photonic Technology) for his first experiments and support.

References

[1] A. Gawlik, I. Höger, J. Bergmann, J. Plentz, T. Schmidt, F. Falk, and G. Andrä, "Optimized emitter contacting on multicrystalline silicon thin film solar cells", Phys. Status Solidi RRL, vol. 9, pp.397–400, 2015.

[2] J. Dore, D. Ong, S. Varlamov, R. Egan, M.A.Green, "Progress in laser-crystallized thin-film polycrystalline silicon solar cells: intermediate layers, light trapping, and metallization, IEEE J. Photov., vol. 4 (1), pp. 33-39, 2014.

[3] G. Jia, G. Andrä, A. Gawlik, S. Schönherr, J. Plentz , B. Eisenhawer, T. Pliewischkies, A. Dellith, F. Falk, "Nanotechnology enhanced solar cells prepared on laser-crystallized polycrystalline thin films (<10 μm)", Sol. Energy Mater. Sol. Cells, vol. 126, pp. 62-67, 2014.

[4] J. Haschke, D. Amkreutz, L. Korte, F. Ruske, B. Rech B, "Towards wafer quality c-Si thin-film solar cells on glass", Sol. Energy Mater. Sol. Cells, vol. 128, pp. 190-197, 2014.

[5] D. Amkreutz, J Haschke, S. Kühnapfel, P. Sonntag, B. Rech, "Silicon thin-film solar cells on glass with open-circuit voltages above 620 mV fromed by Liquid-phase crystallization", IEEE J Photov., vol. 4, pp. 1496-1501, 2014.

[6] P. Sonntag, N. Preissler, M. Bokalič, M. Trahm, J. Haschke, R. Schlatmann, M. Topič, B. Rech and D. Amkreutz, "Silicon Solar Cells on Glass with Power Conversion Efficiency above 13% at Thickness below 15 Micrometer", Scientific Reports, vol. 7 (879), pp. 1-12, 2017.

[7] C. T. Trinh, N. preissler, P. Sonntag, M- Muske, K. Jäger, M. Trahms, R. Schlatmann, B. Rech and D. Amkreutz, "Potential of interdigitated back-contact silicon heterojunction solar cells for liquid phase crystallized silicon on glass with efficiency above 14%", Sol. Energy Mat. Sol. Cells, vol. 174, pp. 187-195, 2018.

[8] G. Jia, A. Gawlik, J. Plentz, G. Andrä, Bifacial multicrystalline silicon thin film solar cells, "Bifacial multicrystalline silicon thin film solar cells", Sol. Energy Mat. Sol. Cells, vol. 167, pp. 102-108, 2017.

[9] C. Battaglia, X. Yin, M. Zheng, I. D. Sharp, T. Chen, S. McDonnell, A. Azcatl, C. Carraro, B. Ma, R. Maboudian, R. M. Wallace and A. Javey, "Hole Selective MoOx Contact for Silicon Solar Cells", Nano Lett., vol. 14, pp. 967-971, 2014.

[10] L. G. Gerling, S. Mahato, A. Morales-Vilches, G. Masmitjà, P. Ortega, C. Voz, R. Alcubilla and J. Puigdollers, "Transition metal oxides as hole-selective contacts in silicon heterojunctions solar cells", Sol.Energy Mater. Sol. Cells, vol. 145, pp. 109-115, 2016.

[11] Gerard Masmitjà, Luís G. Gerling, Pablo Ortega, Joaquim Puigdollers, Isidro Martín, Cristóbal Voz and Ramón Alcubilla, "V2Ox-based hole-selective contacts for c-

Si interdigitated back-contacted solar cells", J. Mater. Chem. A, vol. 5, pp. 9182-9189, 2017.

[12] J. Plentz, T. Schmidt, A. Gawlik, J. Bergmann, G. Andrä, D. Hauschild, V. Lissotschenko, "Applicability of an economic diode laser emitting at 980 nm for preparation of polycrystalline silicon thin film solar cells on glass", Phys. Status Solidi A, vol. 214, pp. 1600882, 2017.

[13] B. Hoex, M.C.M. Van de Sanden, J. Schmidt, R. Brendel, W.M.M. Kessel,"Surface passivation of phosphorus-diffused n+-type emitters by plasma-assisted atomic-layer deposited Al2O3", Phys. Status Solidi RRL, vol. 6, pp. 4-6, 2012.

[14] G. Agostinelli, A. Delabie, P. Vitanov, Z. Alexieva, H.F.W. Dekkers, S. De Wolf, G. Beaucarne, "Very low surface recombination velocities on p-type silicon wafers passivated with a dielectric with fixed negative charge", Sol. Energy Mater. Sol. Cells, vol. 90, pp. 3438–3443, 2006.

[15] G. Lopez, P. Ortega, C. Voz, I. Martín, M. Colina, A. B. Morales, A. Orpella and R. Alcubilla, "Surface passivation and optical characterization of Al2O3/a-SiCx stacks on c-Si substrates", Beilstein J. Nanotechnol., vol. 4, pp. 726–731, 2013.

[16] G. López, C. Jin , I. Martín and R. Alcubilla, "Impact of c-Si Surface Passivating Layer Thickness on n+ Laser-Doped Contacts Based on Silicon Carbide Films", IEEE J. Photov., vol. 8, pp. 976-981, 2018.

[17] C. Jin, I. Martín, G. López, S. Harrison, G. Masmitja, P.R. Ortega and R. Alcubilla, "Silicon solar cells with heterojunction emitters and laser processed base contacts", Energy Procedia, vol. 124, pp. 604-611, 2017.

[18] M. Vetter, G. Lopez, P. Ortega, I. Martin, G. Andrä, D. Muñoz, C. Molpeceres, "Interdigitated laser-contacted solar cell on liquid-phase crystallized silicon on glass", in Proc. of the 27th European Photovoltaic Solar Energy Conference and Exhibition (EUPVSEC), Amsterdam, The Netherlands, 2017, pp. 827-831.

[19] M.A. Green, "Solar cells: Operating principles, technology and system applications", Englewood Cliffs, NJ, USA:Prentice-Hall Inc., 1982, pp. 97.

[20] A. Fell, "A Free and Fast Three-Dimensional/Two-Dimensional Solar Cell Simulator Featuring Conductive Boundary and Quasi-Neutrality Approximations", IEEE Trans. Electron Devices ED-60, pp. 733-738, 2012.

[21] S. Manzoor, Z.J. Yu, A. Ali, W. Ali, K.A. Bush, A.F. Palmstrom, S.F. Bent, M.D. McGehee, Z.C. Holman, "Improved light management in planar silicon and perovskite solar cells using PDMS scattering layer", Sol. Energy Mat. Sol. Cells, vol. 173, pp. 59-65, 2017.

[22] M. Junghanns, J. Plentz, G. Andrä, A. Gawlik, I. Höger and F. Falk, "PEDOT:PSS emitters on multicrystalline silicon thin-film absorbers for hybrid solar Cells", Appl. Phys. Lett., vol. 106, pp. 083904, 2015.

[23] A. Gawlik, J. Plentz, I. Höger, G. Andrä, T. Schmidt, U. Brückner, and F. Falk, "Multicrystalline silicon thin film solar cells on glass with epitaxially grown emitter prepared by a two-step laser crystallization process", Phys. Status Solidi A, vol. 212 (1), pp. 162–165, 2015.

[24] M. Vetter, G. Jia, A. Sanei, A. Gawlik, J. Plentz, G. Andrä, “Evaluation of light trapping structures for liquid-phase crystallized silicon on glass (LPCSG)”, Phys. Status Solidi A, vol. 214, pp. 1600859, 2017.

[25] M. Vetter, A. Gawlik, J. Plentz, G. Andrä, “Carrier lifetime in liquid-phase crystallized silicon on glass”, Energy Procedia, vol. 92, pp. 248-254, 2016.

[26] P. Ortega, G. López, D. Muñoz, I. Martín, C. Voz, C. Molpeceres, R. Alcubilla, “Fully low temperature interdigitated back-contacted c-Si(n) solar cells based on laser-doping from dielectric stacks”, Sol. Energy Mat. Sol. Cells, vol. 169, pp. 107-112 (2017).

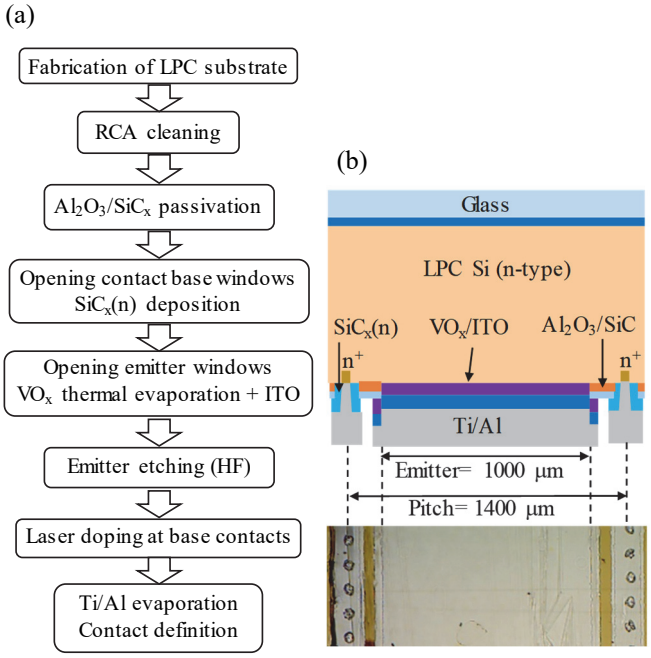

Figure 1.(a) Fabrication process of the solar cells; (b) sketch of the cross-section and microscopic image of the fingers at the final device.

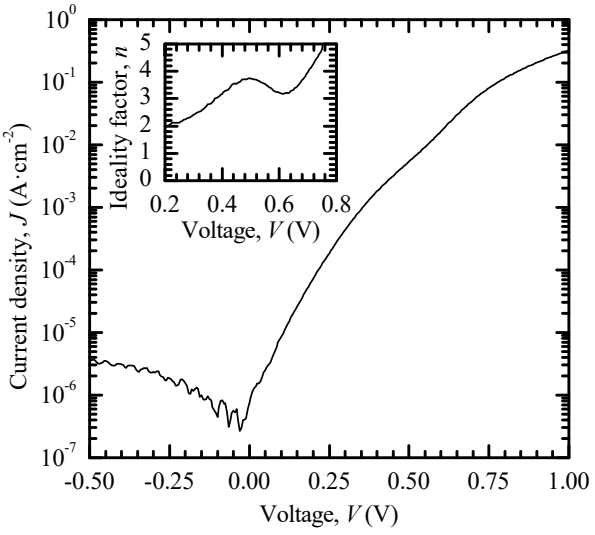

Figure 2. Dark J-V curve of the finished solar cell. (inset) Local ideality factor calculated applying equation (1).

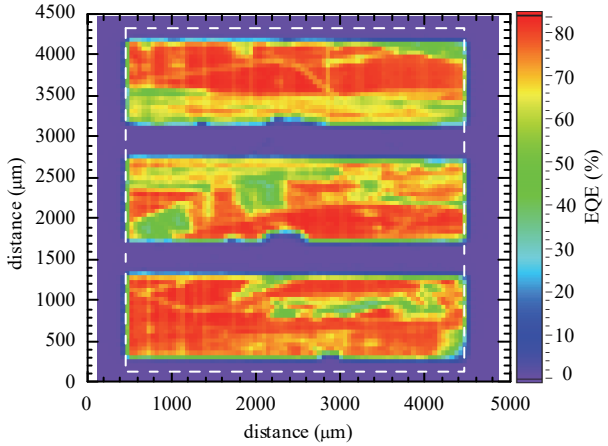

Figure 3. LBIC measurement and EQE mapping of the solar cell. Only the emitter regions are collecting carriers.

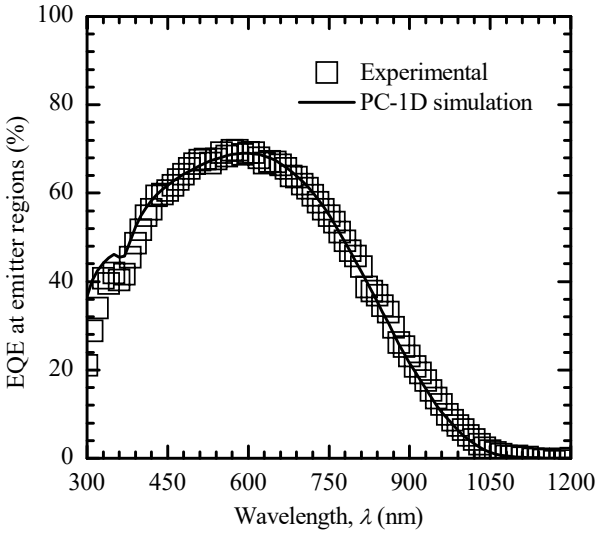

Figure 4. Experimental EQE data at the active area regions (symbols) and PC-1D simulation (line).

Table I. Photovoltaic parameters of the fabricated solar cells under 1 sun-illumination with AM1.5g.

	V_{oc} (mV)	J_{sc} (mA/cm^2)	FF (pFF) (%)	η (%)
Flat glass surface	558	13.62	49.7 (66.1)	3.8
With texturized PDMS	558	14.40	49.6 (66.4)	4.0